AUTOMATED FINE-SCALE FOREST INVENTORY USING BACKPACK LIDAR – A STRATEGY BASED ON FEATURE EXTRACTION, MATCHING, AND TRACKING FROM INTEGRATED SCANS

H. Rastiveis[1,2], T. Zhou[1], C. Zhao[1], S. Fei[2], and A. Habib[1]*

[1]Lyles School of Civil Engineering, Purdue University, West Lafayette, USA - (hrasti, zhou732, zhao1259, ahabib)@purdue.edu
[2] Department of Forestry and Natural Resources, Purdue University, West Lafayette, USA - sfei@purdue.edu

KEY WORDS: Trajectory Enhancement, Mobile Mapping Systems, Backpack LiDAR, Diameter at Breast Height (DBH), Tree Biometric Extraction.

ABSTRACT:

Backpack LiDAR systems are gaining popularity due to their rapid data acquisition, portability, and cost-effectiveness. However, using backpack LiDAR in forest poses challenges, such as GNSS signal attenuation under the canopy, leading to inaccurate trajectory estimates and misregistered point clouds. This paper aims at presenting a novel method that addresses this challenge by leveraging the integrated scans (IS) concept to enhance point cloud quality for automated forest inventory. The proposed method for forest inventory using ISs consists of four key steps: (i) Integrated scans (IS) generation, (ii) feature extraction, matching, and tracking, (iii) trajectory enhancement, and (iv) tree biometric extraction. Firstly, IS point clouds are generated based on the initial GNSS/INS trajectory. Secondly, reliable forest features such as tree trunks and ground patches are extracted, matched, and tracked across ISs. These features are then utilized in the trajectory enhancement step, where a non-linear Least Squares Adjustment (LSA) technique is used to minimize discrepancies among the features to enhance the trajectory. The resulting point clouds, based on the improved trajectory, are used to extract tree biometric information. The proposed method was evaluated using two distinct datasets collected with different systems. The evaluation results, both qualitatively and quantitatively, validate the effectiveness of the proposed method, showcasing its potential for fine-scale forest inventory applications.

1. INTRODUCTION

1.1 Significance and Motivation

Forests play a pivotal role as a vital natural resource, offering a wide range of ecological, economic, and social benefits. The forest industry significantly contributes to the economy of many countries, generating employment opportunities, income, and valuable products like timber and paper (Baldrian et al., 2023). Forest inventory holds immense importance in achieving these objectives, as it enables forest managers and policymakers to acquire precise and comprehensive information about forest resources. This includes vital aspects such as the volume and density of trees, as well as ecological parameters like biodiversity and carbon storage (Maitreya et al., 2023). Accurate estimation of tree volume and biomass is particularly crucial, as inaccuracies can lead to adverse consequences such as overharvesting or underutilization of forest resources. These scenarios result in economic losses and environmental damage (Shu et al., 2023).

Traditionally, forest inventory has relied on manual methods, which are both time-consuming and labor-intensive. As a more efficient alternative, remote sensing technologies like LiDAR have emerged as valuable tools for conducting forest inventory (Beland et al., 2019). Among these technologies, airborne LiDAR has been widely utilized to gather crucial information on forest structure and biomass estimation (Kelly and Di Tommaso, 2015). However, its resolution may not be sufficient to extract detailed biometric information such as Diameter at Breast Height (DBH) and height. Studies conducted by Novotny et al. (2021) have pointed out the limitations of airborne LiDAR in accurately deriving DBH measurements. To overcome these limitations and acquire fine-scale biometric information, researchers have shifted their focus to Uncrewed Aerial Vehicle (UAV) LiDAR systems. UAV LiDAR offers higher resolution and enhanced flexibility in capturing detailed forest information, as demonstrated by Corte et al. (2020). However, even with improved resolution, UAV LiDAR may still have limitations when it comes to fine-scale forest inventory. To tackle this challenge, alternative technologies like portable (either handheld or backpack) LiDAR systems have emerged. These systems are cost-effective and capable of providing high-resolution point clouds within a forest (Su et al., 2020). Among the portable LiDAR systems, the backpack LiDAR is particularly popular and represents a viable alternative for forest inventory applications, enabling more accurate and efficient data collection compared to traditional manual methods.

1.2 Problem Statement and Research Objectives

A backpack LiDAR usually is composed of a laser scanner to collect 3D points, a camera(s) for image acquisition, and a Global Navigation Satellite System (GNSS) aided by Inertial Navigation System (INS) to provide the positional and orientational parameters of the system. In a such a system, the mathematical model for determining the 3D coordinates of an object point in the mapping frame r_o^m is expressed by Equation (1) (Zhou et al., 2023):

$$r_o^m(t) = r_{b(t)}^m + R_{b(t)}^m r_{lu}^b + R_{b(t)}^m R_{lu}^b r_o^{lu(t)} \quad (1)$$

where, variables are defined as follows:

- $r_{b(t)}^m$ and $R_{b(t)}^m$represent the position and orientation information of the GNSS/INS body frame coordinate system relative to the mapping frame at the time of scanning (t).

- r_{lu}^{b} and R_{lu}^{b}denote the lever arm and boresight rotation matrix that establish the relationship between the laser unit system and GNSS/INS body frame.
- $r_{o}^{lu(t)}$ is derived from raw LiDAR measurements at the time of firing and represents the position of the laser beam footprint relative to the laser unit frame.

Under ideal conditions with no noise, where all parameters in the right-hand side of the Equation (1) are accurately known, the coordinates of objects in the mapping frame can be calculated with high precision, ensuring no misalignment between points. Consequently, an object point observed at different times would maintain the same coordinates in the mapping frame. However, in environments with a weak GNSS signal, such as densely forested areas, the accuracy of point cloud generation is compromised, leading to misalignments. This is particularly pronounced as the position and orientation of the GNSS/INS body frame ($r_{b(t)}^{m}$ and $R_{b(t)}^{m}$) rely on GNSS and INS measurements. This paper proposes a novel solution for this problem aimed at enhancing trajectory accuracy and generating high-quality point clouds with minimized misalignments. The resulting point clouds will be utilized in forest inventory.

1.3 Review of Existing Literature

To address the aforementioned problem, researchers have explored various approaches, particularly focusing on Simultaneous Localization and Mapping (SLAM) aided positioning solutions. For instance, Tang et al. (2015) utilized point clouds from a small-footprint LiDAR to estimate the orientation parameters of the system trajectory. Their SLAM/INS trajectories yielded superior 2D tree stem positions compared to GNSS/INS trajectories. However, their approach only estimated orientational parameters, neglecting positional trajectory estimation. Additionally, while the achieved accuracy was suitable for tree stem localization, it fell short in accurately estimating tree biometric information such as DBH. Qian et al. (2016) enhanced the positional accuracy of their LiDAR-based SLAM by incorporating heading angles and velocities from GNSS/INS. Their method showed promising results in feature-rich forests but might not perform well in open forests with sparse trees. Kukko et al. (2017) proposed a trajectory enhancement strategy that involved generating point clouds from a short time period using the initial GNSS/INS trajectory, and correcting the trajectory based on centroids of the tree trunk slice at 3–3.5 m height from ground. Relying solely on tree trunk centroids in their method, may result in weak vertical control for trajectory enhancement. Chiella et al. (2019) employed Attitude and Heading Reference Systems (AHRS) and 2D LiDAR odometry in conjunction with GNSS information. They derived the platform's motion through a scan matching algorithm based on tree trunks. However, their method was designed for 2D LiDAR and cannot handle 3D LiDAR data.

Su et al. (2020) developed a GNSS-free BP LiDAR system with two LiDAR units. They implemented a LiDAR-based SLAM approach to estimate the trajectory's position and orientation parameters and extract tree biometric information in forest. The reported accuracy for estimated height and DBH were 2.24 m and 0.03 m, respectively. However, their LiDAR-SLAM strategy required manual corrections in complex natural forests. Similarly, Ramezani et al. (2022) proposed the Wildcat strategy for trajectory estimation, which relied solely on the Inertial Measurement Unit (IMU) information of a robot equipped with a LiDAR system. Their method consisted of two key modules: Wildcat odometry and pose-graph optimization (PGO). The Wildcat odometry module integrated asynchronous IMU and LiDAR measurements to address map distortion caused by sensor motion. The PGO module optimized the robot trajectory and environment map globally. While the GNSS-free methods provided reasonable accuracy, the resulting point clouds were not georeferenced, making multi-temporal data acquisition and forest monitoring challenging. Zhou et al. (2023) proposed a state-of-the-art method that extracted tree trunks and ground patches from LiDAR scans and enhanced the trajectory by minimizing discrepancies between corresponding features. Although they reported promising results, their method was tested primarily on plantation forests and may not be feasible for natural forests with dense canopy. Additionally, their feature extraction relied on single LiDAR scans, which poses challenges such as sparsity of the point clouds.

1.4 Contribution

Based on the findings from previous studies, it is evident that there is still potential for improving the accuracy and efficiency of using backpack LiDAR for forest inventory in challenging environments with weak GNSS signals.

It should be noted that while the absolute accuracy of the GNSS/INS trajectory may be unreliable in such environments, its relative accuracy over a short period remains reasonable. Therefore, in this paper, we propose a novel strategy that utilizes IS point clouds to extract features for trajectory enhancement. An IS point cloud refers to the combination of multiple LiDAR scans acquired within a short time period. In this context, each LiDAR scan refers to the points from a full revolution of the laser beams. The utilization of IS offers several advantages, primarily enabling the extraction of more reliable features compared to using a single LiDAR scan. This addresses the challenge of feature extraction from LiDAR point clouds in complex environments. Additionally, our methodology introduces an automated tree trunk extraction process from LiDAR point clouds. Furthermore, we investigate the automated extraction of tree biometric information such as DBH and height for fine-scale forest inventory in natural forest settings.

2. METHOD

The flowchart presented in Figure 1 depicts the proposed strategy for fine-scale forest inventory using backpack LiDAR. It showcases the input components of individual LiDAR scans, GNSS/INS trajectory, and system calibration parameters, while the output of this strategy is the tree biometric information in the forest.

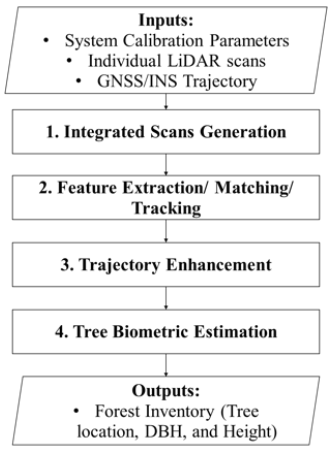

Figure 1. Flowchart of the proposed method for fine-scale forest inventory from Backpack LiDAR point clouds

To accomplish this, the first step involves generating integrated scans by utilizing the initial GNSS/INS trajectory. Subsequently, reliable forest features are extracted, matched, and tracked across different integrated scans, constituting the second step. These extracted features are then fed into the third step, trajectory enhancement, where a Least Squares Adjustment (LSA) technique is employed to minimize discrepancies among features captured at different timestamps while considering the absolute and relative positional/rotational information provided by the GNSS/INS trajectory. The output of the third step is an enhanced trajectory that is utilized to generate the improved point clouds. The resulting point clouds are then used to extract tree biometric information.

2.1 IS Generation

The generation of IS point clouds involves combining multiple LiDAR scans within a defined time period. The IS length, or the number of scans, is a crucial parameter. Shorter IS lengths result in point clouds with reduced misalignment due to scans acquired closely in time. However, feature extraction may be less accurate due to limited coverage and low-density point clouds. Longer IS lengths improve feature extraction reliability with more comprehensive coverage but may increase misalignment and pose challenges for extraction.

Through a trial-and-error process, it has been determined that using 100 scans as the IS length make the feature extraction and minimized misalignment. Considering that our LiDAR scanning rate is 10 scans per second, collecting 100 scans corresponds to a data acquisition duration of 10 seconds. Within this duration, the object points are assumed to have a reasonable alignment. Figure 2 provides a visual representation of the resulting point clouds obtained from different IS length. By selecting an appropriate IS length, in this case, 100 scans, we aim to strike a balance between reducing misalignment and ensuring accurate feature extraction. Figure 2 visually demonstrates the resulting IS point clouds considering different IS lengths. The analysis of Figure 2 reveals that in the point cloud generated from a single LiDAR scan (Figure 2-a), forest features appear unclear and challenging to extract. Moreover, when using 7500 LiDAR scans (Figure 2-d), different versions of objects are observed, making object extraction a difficult task. However, when a limited number of scans are employed to generate point clouds (as depicted in Figure 2-b and 2-c), forest features such as tree trunks become more discernible.

Figure 2. Generated point clouds of a Backpack LiDAR using different IS Length in a forest; (a) One scan, (b) 100 scans, (c) 500 scans, (d)7,500 scans.

2.2 Feature Extraction, Matching, and Tracking:

The second step of the process focuses on the extraction, matching, and tracking of reliable features, specifically tree trunks and ground patches, across different ISs. Tree trunks are modeled as cylindrical features to provide horizontal control and ground patches are used as plane features to provide vertical control. To extract these features, initially, the modified Cloth Simulation Filter (mCSF) (Shin et al., 2023) is employed to derive a Digital Terrain Model (DTM) for each IS. Considering a 0.2m for bare-earth threshold, the points are then divided into above-ground and bare-earth points, which are utilized for tree trunk and ground patch extraction, respectively.

2.2.1 Tree Trunk Extraction: The extraction of tree trunks from the above-ground point cloud relies on the fact that tree trunks exhibit a higher local density compared to their surroundings. Therefore, to extract tree trunks, a density image of the above-ground points is generated, considering a pixel size of 0.5m. Importantly, the density image generation process involves the utilization of points within the height range of 0.5m to 5m. Once the above-ground points have been normalized using the DTM obtained from the mCSF, these points are extracted. The peak points on this image indicate the potential locations of tree trunks. This study suggests employing the Otsu's thresholding method (Otsu, 1979). However, tree trunks within an IS may exhibit different densities. Hence, an iterative technique is utilized to identify all peak points on the density image. In each iteration, a threshold is determined using the Otsu's thresholding technique to detect high-density points, which correspond to the peak points. For each peak location, a 3D line is fitted to the points to determine the orientation of the tree. Then, all points within a predefined threshold distance (e.g., 0.5m) from the fitted line are selected as tree trunk points. It is important to note that false positive tree trunks are identified by examining the continuity of the points along the height direction. Continuity is assessed by slicing the points in the Z direction and calculating the Coefficient of Variation (CV) index, as shown by Equation 2:

$$\mathrm{CV} = \frac{Std_{\mathrm{SP}}}{Mean_{\mathrm{SP}}} \qquad (2)$$

Here, Std_{sp} and $Mean_{sp}$ represent the standard deviation and mean of the number of points in the slices, respectively. A lower CV value indicates similar numbers of points in the slices, confirming the true tree trunk. Conversely, a higher CV value suggests discontinuity, indicating a false positive tree trunk. In this research, a slice interval of 0.25m is considered. Additionally, unwanted points, such as branch points, are eliminated by fitting a circle to all extracted tree trunk points and employing an outlier removal technique. The Interquartile Ranges (IQR) method is utilized during the outlier removal step (Vinutha et al., 2018). Figure 3-a illustrates the extracted tree trunk feature from a sample of integrated scans. Moreover, to address the issue of over-segmentation during tree extraction, a merging operation is applied to close trees with a distance of less than 0.5m. The selection of this value can be based on the minimum distance observed between trees in the specific area.

2.2.2 Tree trunks matching and tracking: Once all tree trunks are extracted from the ISs, they are then matched in successive ISs based on their spatial and orientation proximity. In other words, if the distance between tree locations in successive ISs is less than the proximity threshold, and the angle between their fitted line is less than an orientation threshold, they are considered as matched trees. Here, a 0.7m and a 10o values were used as the spatial and orientation thresholds, respectively. The parameters were carefully chosen through a trial-and-error process. It is noteworthy to mention that the orientation thresholds contribute to ensuring that each section of the v-shaped tree trunk is extracted as an individual feature. Detecting matched trees between consecutive ISs, the relative 2D

transformation parameters are obtained. This is an iterative process where matched tree trunks are used to refine the relative transformation parameters, which in turn are used for the next iteration of the tree trunk matching. Eventually, tree trunks can be tracked in all ISs.

2.2.3 Ground Patch Extraction: A ground patch is defined as a small cluster of neighboring points within a given search radius (e.g., 1 m) at a known location on the ground surface. The points of a ground patch are used as plane feature. The ground patches are extracted from the bare-earth point clouds generated by the mCSF. To determine the locations of the ground patches in different ISs, a grid of seed points is initially generated across the area, with a specified interval grid size (e.g., 3 m). The initial seed points' locations are used to extract ground patches from the first IS. However, to establish the corresponding ground patch locations in the subsequent ISs, the transformation parameters between consecutive ISs, which are obtained during the "tree matching and tracking" step, are utilized. This enables the transfer of seed point locations from one IS to the next, and this process continues until the seed point locations in the last IS are determined. With the seed point locations available for all ISs, ground patches are then extracted from the bare-earth point clouds. Figure 3-b showcases an example of the extracted ground patches from a sample IS.

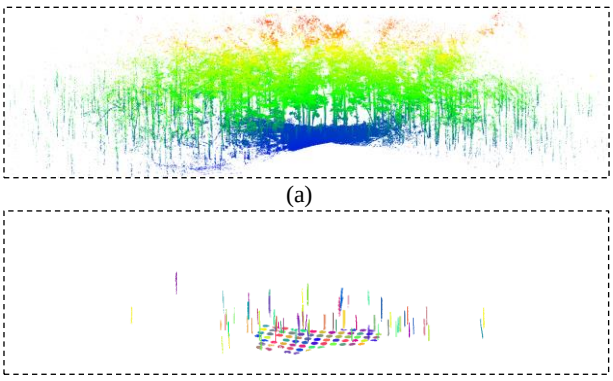

(a)

(b)

Figure 3. Extracted features from a sample IS. (a) the sample IS colored by height; (b) extracted tree trunk and ground patches colored by feature ID.

It is important to mention that in order to eliminate noisy points from the ground features, a plane is fitted to each ground patch, and points with a distance larger than 0.1m from the fitted plane are removed. Furthermore, a threshold for the number of points within each ground patch is considered to discard small ground patches. The ground patches close to the trajectory usually include so many redundant points. Threfore, a downsampling procedure for such ground patch is helpful to improve the efficiency.

2.3 Trajectory Enhancement

After extracting all tree trunks and ground patches, eventually, they are fed into a trajectory enhancement procedure to improve the quality of the GNSS/INS trajectory and point cloud alignment. This enhancement method leverages LSA to determine optimal values for positional and orientational parameters of the sensor at each timestamp. The optimization process involves minimizing the normal distance between LiDAR points and corresponding parametric models for cylindrical and planar features. It is important to note that this paper does not delve into the detailed description of the optimization framework. However, a general description of this step is described in this subsection. Interested readers are encouraged to refer to (Zhou et al., 2023) for more comprehensive insights into the LSA-based trajectory enhancement using cylindrical and planar features.

Equation (1), which represented the fundamental point positioning equation, is used as the basis for this LSA-based optimization framework. By considering the estimated corrections to positional and orientation parameters as $\delta r^m_{b(t)}$ and $\delta R^m_{b(t)}$, Equation (3) defines the corrected point position:

$$r_o^m(t)_{corrected} = f(r^m_{b(t)}, \delta r^m_{b(t)}, R^m_{b(t)}, \delta R^m_{b(t)}, r^b_{lu}, R^b_{lu}, r_o^{lu(t)}), \quad (3)$$

The optimization framework simultaneously determines optimal values for trajectory position and orientation parameters, as well as parameters describing the feature models. Cylindrical models in 3D space are defined by three direction parameters (u_x, u_y, u_z), three location parameters representing a point on the axis (x_0, y_0, z_0), and a radius (r) while planes are defined by four parameters: three normal vector parameters (n_x, n_y, n_z) and the distance to the origin (d). Additionally, since the obtained trajectory is relatively smooth, it undergoes downsampling based on a predefined time interval. The down-sampled trajectory points, referred to as reference points, are then used to interpolate other trajectory points. For this research, a time interval of 1 second and a 2nd order polynomial interpolation method using three neighboring reference points are applied for downsampling and interpolation, respectively. Once the enhanced trajectory is obtained, new point clouds generated from the area are utilized for extracting tree biometric information.

2.4 Tree Biometric Information Estimation

In this research, DBH and tree height are extracted as two significant biometric information, in addition to tree location. This step initiates with a statistical noise removal procedure aimed at mitigating the impact of noisy points on the estimation. Subsequently, the method described in Section 2.2.1 is employed on the enhanced point clouds to extract the tree trunks. Then, points within the height range of 1.3 to 1.5 m are selected from each tree trunk to estimate the DBH. This estimation is accomplished by fitting a circle to these points using the LSA method. It should be noted that the outliers are removed during the circle fitting. The center of the fitted circle serves as the tree's location, while twice the fitted radius is considered the estimated DBH. Once all tree locations have been determined, a Voronoi tessellation is employed to extract tree boundaries for height estimation (Safaie et al., 2021). In this case, the difference between the maximum and minimum Z coordinate of the points within the boundary of each tree is taken as the tree's height.

3. EXPERIMENTS AND RESULTS

3.1 Study Area and Sensor Specifications

In this study, we conducted a comprehensive evaluation of the proposed forest inventory strategy using data acquired from Martell Forest Plot 4D, located in West Lafayette, Indiana, USA. The study area consists of a diverse range of tree species, including black oak (*Quercus velutina*), white oak (*Q. alba*), yellow poplar (*Liriodendron tulipifera*), ash (*Fraxinus* spp.), basswood (*Tilia americana*), and sugar maple (*Acer saccharum*). The forest comprises a mixture of large, mature trees, as well as young and vigorous small saplings resulting from a previous

regeneration event. The understory vegetation encompasses both native and invasive shrubs, covering a substantial portion of the study area. The average DBH for adult trees is approximately 300 mm. For our study, we collected two datasets on October 19th, 2022 (OCT22 dataset), and March 2nd, 2023 (MAR23 dataset) with 29- and 13-minutes collection time, respectively. Figures 4-a and 4-c provide an overview of the selected test area and depicts the corresponding trajectories for each dataset. Furthermore, Figure 4-b offers a visual representation of the study area's interior during the collection of the first dataset, showcasing the presence of shrubs, young trees, and mature trees.

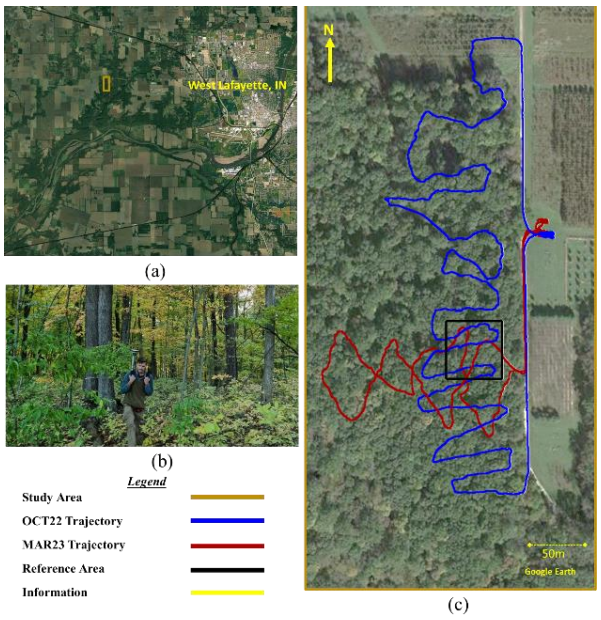

Figure 4. Overview of the selected study area. (a) location of the plot4d of the Martell Forest in West Lafayette, IN; (b) study area's interior during OCT22 dataset collection; (c) overview of the trajectories in OCT22 and MAR23 datasets.

The datasets were collected using two in-house developed backpack LiDAR in our research group called CPT_VLP16HR and E2_HDL32E. Utilizing these systems, totally 440 and 423 million points were collected for OCT22 and MAR23 datasets, respectively. The specifications of these systems are summarized by Table (1).

3.2 Results

Total number of scans in OCT22 and MAR23 datasets were 17,400 and 7500, respectively. Therefore, considering 100 scans for the integrated scans length, 174 and 75 ISs were generated for processing these datasets. From each datasets the tree trunks and ground patches were extracted, matched, and tracked. The extracted features were fed into the trajectory enhancement step. Figure 5 shows part of the extracted cylindrical (tree trunks) and planer (ground patches) features before and after the optimization for the MAR23 dataset. As can be seen from this figure, the misalignment between the feature points are successfully removed. Table 2 presents a summary of the trajectory enhancement in both datasets.

After implementing the trajectory enhancement, DBH and height of the trees in both datasets was estimated. Figure 6 presents a 3D visualization of the extracted trees, with each tree depicted in a random color. The black color represents the 20cm section points used for circle fitting, while the fitted circles are highlighted in red.

			CPT_VLP16HR (OCT22 dataset)	E2_HDL32E (MAR23 dataset)
				
Camera Unit	Camera Model		Sony α7R II	Sony α6000
	Camera Type		RGB Frame Camera	RGB Frame Camera
	Focal Length		28 mm	16 mm
	Image Dimensions		7952 x 5304 pixels	6000×4000 pixels
	Pixel Size		4.50 µm	3.88 µm
	Wavelength Range		400-700 nm	400-700 nm
Laser Unit	LiDAR Model		Velodyne VLP-16 HR	Velodyne HDL 32E
	#Channels		16	32
	Field of View		Horizontal: 360° Vertical: -10° to +10°	Horizontal: 360° Vertical: -30.67° to +10.67°
	Range		100 m	100 m
	Ranging Accuracy		±3 cm	±2 cm (avg.)
	#Points/sec		300,000	695,000
GNSS/INS Unit	GNSS/INS Model		SPAN-CPT	PwrPak7-E2
	Accuracy After 0s, 10s, and 60s outrage	Positional Horizontal	1cm, 2cm, 23cm	1cm, 2cm, 17cm
		Positional Vertical	2cm, 2cm, 11cm	2cm, 2cm, 6cm
		Rotational Roll/Pitch	0.008°, 0.008°, 0.013°	0.005°, 0.005°, 0.005°
		Rotational Heading	0.035°, 0.035°, 0.038°	0.01°, 0.01°, 0.012°

Table 1. Technical specifications of the backpack LiDAR systems in OCT22 and MAR23 datasets**.**

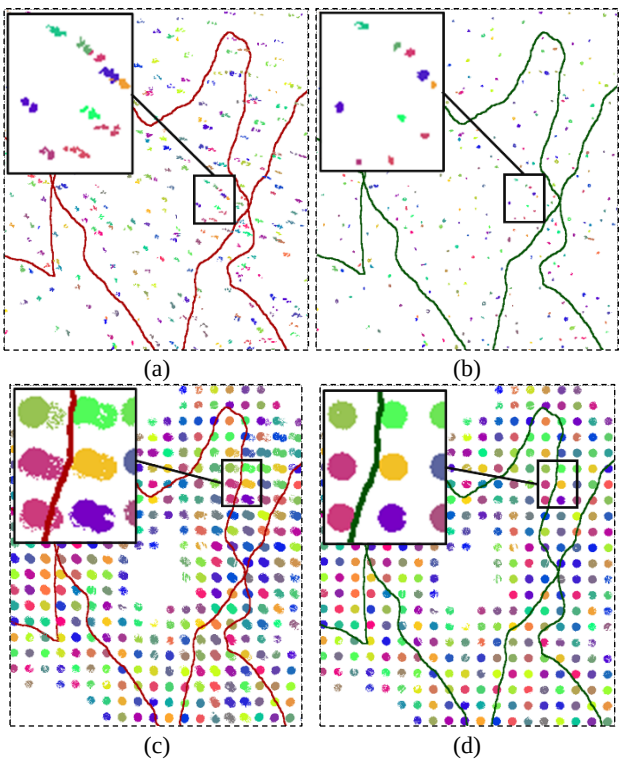

Figure 5. Part of the extracted tree trunk and ground patches used in the trajectory enhancement of the MAR23 dataset; Red line is the initial GNSS/INS trajectory, green line is the enhanced trajectory; Points are colored by feature ID. (a) and (c) before the trajectory enhancement; (b) and (d) after the trajectory enhancement.

Dataset		OCT22		MAR23	
# ref. points		2,828		1,483	
# plane features		1568		903	
# cylinder features		1803		906	
# points		20,325,100		10,095,952	
factor variance ratio		1.017		0.7643	
Corrections to the GNSS/INS trajectory	Statistics	Mean	Std	Mean	Std
	X(m)	-0.0087	0.6378	0.0337	0.5064
	Y(m)	-0.0299	0.6891	-0.0056	0.2651
	Z(m)	-0.0464	1.4298	-0.0571	0.5808
	ω(deg)	0.0009	0.0921	-0.0008	0.0119
	φ(deg)	0.0019	0.0847	0.0013	0.0118
	κ(deg)	0.0030	0.4018	0.0238	0.1099

Table 2. Summary of the LSA-based trajectory enhancement in OCT22 and MAR23 datasets.

Figure 6. Tree extraction and DBH estimation results using LSA-based circle fitting. Extracted trees are displayed in random colors, selected points for circle fitting are shown in black, and the fitted circles are highlighted in red.

Figure 7 showcases the LSA-based fitted circles for three sample trees, displaying the inlier and outlier points in red and blue, respectively. This visualization demonstrates the successful removal of outliers from the data points, resulting in reasonable fitted circles. Furthermore, DBH and height heat maps are useful representation of a forest inventory data. Figure 8 shows the resulting heat map of the DBH and height of a small area of our study site using the MAR23 dataset.

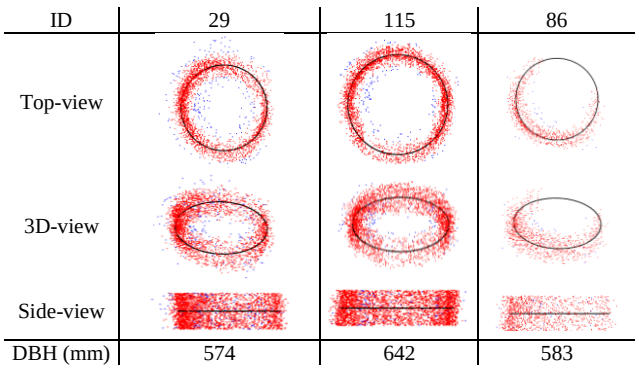

Figure 7. LSA-based circle fitting results for three sample trees in the MAR23 dataset. Fitted circles is depicted in black, inlier points are marked in red and outlier points are indicated in blue.

3.3 Accuracy Assessment

To assess the performance of the proposed strategy for fine-scale forest inventory using backpack LiDAR, both qualitative and quantitative evaluations were conducted. In the qualitative evaluation, the enhanced point clouds obtained after trajectory enhancement were compared to the point clouds generated using the GNSS/INS trajectory. In addition, the generated point clouds from a commercial backpack LiDAR system (Hovermap, https://emesent.com), which collected data through the same trajectory as the MAR23 dataset, were used in the evaluation. Figure 9-a displays a side-view of the generated point clouds for a small profile of the study area and the top-view of a 20cm section of points based on the initial GNSS/INS of the MAR23 dataset. The misalignment between points is clearly seen in this Figure. Also, the improved point clouds for both datasets and the commercial backpack LiDAR are shown in Figure 9-b, 9-c, and 9-d. These figures clearly demonstrate the successful removal of misalignment between tree trunk points, resulting in reasonable tree trunk shapes.

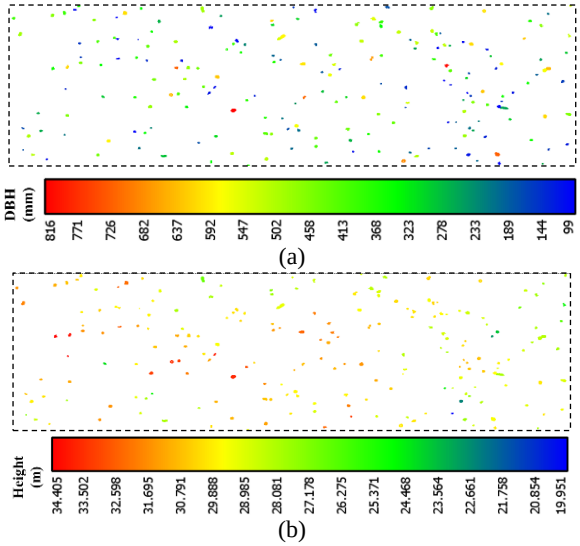

Figure 8. Individual tree locations colored by DBH and height: (a) estimated DBH; (b) estimated height.

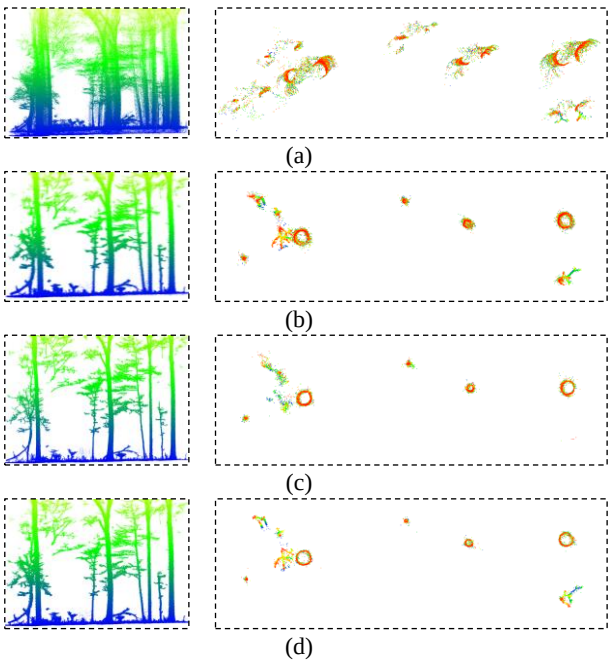

Figure 9. Qualitative evaluation of the improved point clouds; Left: side-view of a small area colored by height. Right: top-view of a 20cm section points in the same area. (a) generated point clouds using the initial GNSS/INS trajectory; (b) improved point clouds in OCT22 dataset; (c) improved point clouds in MAR23 dataset; (d) generated point clouds by a commercial backpack LiDAR used in the same trajectory of the MAR23 dataset.

To assess the quantitative performance of the point clouds, the estimated DBH derived from the improved point cloud data was compared against manually measured ground truth values in the reference area, represented by a black square in Figure 4. In this area, the DBH of 63 trees was measured manually using a tape measure, while their heights were estimated from UAV LiDAR point clouds collected in the same day of the OCT22 dataset. By comparing the estimated DBH and height with the reference data values, we calculated the mean, standard deviation, and Root Mean Square Error (RMSE) of the differences for each dataset, as summarized in Table 3.

	DBH (mm)			Height (m)		
	Mean	**Std**	**RMSE**	**Mean**	**Std**	**RMSE**
OCT22	-26.7	23.2	35.3	-0.5	0.6	0.8
MAR23	4.8	27.0	27.4	-1.0	0.5	1.1
Commercial Sensor	-3.1	17.7	18.0	-0.5	0.3	0.5

Table 3. Accuracy assessment of the estimated DBH and heights using the enhanced point clouds.

As can be seen from Table 3, the MAR23 dataset produced more accurate results compared to the OCT22 dataset. This superiority can be attributed to three main reasons. Firstly, when examining Figure 4, it becomes apparent that the trajectory of the MAR23 dataset had four loops, which potentially facilitated better adjustment and control compared to the trajectory of the OCT22 dataset. Secondly, the MAR23 dataset is a leaf-off dataset, meaning that the GNSS signal is stronger compared to the OCT22 dataset. As a result, the initial GNSS/INS trajectory quality in the MAR23 dataset is higher than that of the OCT22 dataset. This higher quality trajectory serves as a foundation for more accurate data processing and analysis. Additionally, the density of the points collected by the E2_HDL32 backpack system used in the MAR23 dataset is double that of the CPT_VLP16 system used in the OCT22 dataset. Therefore, in addition to the greater number of observations during the trajectory enhancement using the LSA method, the higher point density in the MAR23 dataset contributes to more accurate estimation of the DBH. On the other hand, the height information used as a reference in this study was obtained from UAV data collected on the same day as the OCT22 dataset, during the leaf-on season. The time disparity between the MAR23 and the reference datasets might explain the higher values of RMSE and Std of the height estimation errors of this dataset in Table 3.

4. DISCUSSION

4.1 Processing Time

The proposed forest inventory strategy was implemented in C++ and Python environments. The feature extraction, matching, and tracking steps, as well as tree biometric information extraction, were implemented in Python while the IS generation and trajectory enhancement steps were developed in C++. The code was executed on a computer with an Intel(R) Xeon(R) W-2133 3.60GHz CPU and 64GB of RAM. The processing time for the OCT22 and MAR23 datasets was approximately 5.5 and 4.5 hours, respectively. It is important to note that the LiDAR scanner of the E2_HDL32E sensor used for collecting the MAR23 dataset is the Velodyne HDL32E, which is a 32-channel LiDAR. On the other hand, the OCT22 dataset was collected using a 16-channel sensor. As a result, the number of points collected by the MAR23 dataset's sensor would be twice that of the OCT22 dataset's sensor for the same period. This explains why the processing time for both datasets is close, even though OCT22 dataset having a longer data duration. It is worth mentioning that the most time-consuming part of our implementation is the trajectory enhancement, where millions of observations are used to optimize unknown parameters using a non-linear LSA method. The processing time of this step was 4 and 3 hours for OCT22 and MAR23 datasets, respectively.

4.2 Parameter Setting

Several parameters were carefully selected and used in this strategy for fine-scale forest inventory. For instance, the integrated scan length was set to 100 scans, which represents approximately 10 seconds of data. Increasing this parameter would lead to fewer ISs being generated and reduce processing time. However, it would also result in increased misalignment between object points. Consequently, the location and orientation of the extracted tree trunks over ISs may undergo significant changes, potentially causing the algorithm to fail in matching trees between consecutive ISs. Furthermore, the proximity and orientational thresholds were predefined as 0.7m and 10°, respectively. Modifying these thresholds to larger values may lead to incorrect matches between closely located trees and under segmentation of tree-trunk features. Conversely, smaller values may cause failing in matching corresponding trees in successive scans and lead to an over-segmentation issue, where the tree trunks are labelled several times excessively. Figure 10 demonstrates two sample matching and tracking results. In Figure 10-b, it is observed that a tree trunk is extracted as two distinct features. Nevertheless, due to the relatively lower number of these features compared to the successful matching and tracking results, the final enhanced point clouds show promising.

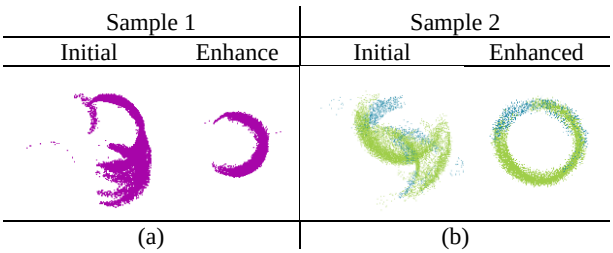

Figure 10. Sample tree trunk matching and tracking results. (a) Successful matching results. (b) Over-segmentation issue sample

During the tree trunk extraction process, a pixel size of 0.5 m was used to generate the density image. This value was determined based on the minimum distance between trees in the area under consideration. While a smaller value may exacerbate the over-segmentation problem, the subsequent merging step implemented after tree trunk extraction effectively addresses this issue.However, it is worth noting that a smaller value would increase computational costs. Conversely, a larger value may cause an under-segmentation problem, where tree trunks are not adequately separated. Besides, merging close trees with a distance of less than 0.5m to tackle the over-segmentation problem may not work well in younger stands. However, the results obtained from tree trunk extraction across multiple ISs during the feature extraction and tree biometric extraction steps demonstrated the reliability of this selected value for tree extraction from backpack LiDAR point clouds in natural forest areas.

4.3 Challenges and Future Works

One of the primary challenges encountered in the trajectory enhancement step is the relatively slow processing speed related to the data collection time. While the method shows promise when compared to manual forest inventory, there is still room for

improving its efficiency. Downsampling the features of the initial integrated scans can be explored to enhance speed, albeit at the cost of potentially reducing the number of observation points.

The mCSF algorithm plays a crucial role in distinguishing between bare-earth and above-ground points. Any error in this algorithm can result in incorrect normalization, leading to the extraction of different sections of tree trunks from different integrated scans. Furthermore, in cases where no ground points are present, the lower portion of the measured tree trunk might be erroneously identified as bare-earth points. Therefore, in our implementation, we disregard ground patches located on a tree trunk.

Another challenge of the proposed algorithm is the occurrence of under-segmentation and over-segmentation errors during tree trunk extraction, matching, and tracking. Although these errors comprise less than 0.5% of the extracted features and can be disregarded, they can still be detected and eliminated from the features to improve accuracy.

5. CONCLUSIONS

This paper presents a novel strategy for fine-scale forest inventory utilizing backpack LiDAR point clouds. The proposed method incorporates tree trunks and ground patches extraction, matching, and tracking techniques across integrated scans. The effectiveness of the approach was evaluated using two datasets collected by different sensors and through distinct trajectories within a natural forest area. The evaluation, both qualitatively and quantitatively, demonstrated notable advancements in terms of trajectory and point cloud quality, as well as the accuracy of estimated tree biometrics.

One significant contribution of this paper is the utilization of IS, which enables reliable extraction of forest features from backpack point clouds. However, it is acknowledged that there is room for improvement in terms of processing efficiency. Future work will focus on enhancing the quality of extracted features between integrated scans to further refine the results. Additionally, exploration of extracting additional features such as tree branches will be undertaken to expand the capabilities of the proposed method.

ACKNOWLEDGEMENTS

The authors would like to express their gratitude to Center for Digital Forestry at Purdue University for providing support for this research. Funding for this research is partially supported by USDA NIFA # 2023-68012-38992. Additionally, they would like to extend their thanks to all the members of the Digital Photogrammetry Research Group (DPRG) and Natural Resources Spatial Analysis (NRSA) labs at Purdue University for their valuable assistance throughout the project.

REFERENCES

Baldrian, P., López-Mondéjar, R., Kohout, P., 2023. Forest microbiome and global change. Nature Reviews Microbiology, 1-15.

Beland, M., Parker, G., Sparrow, B., Harding, D., Chasmer, L., Phinn, S., Antonarakis, A., Strahler, A., 2019. On promoting the use of lidar systems in forest ecosystem research. Forest Ecology and Management 450, 117484.

Chiella, A.C., Machado, H.N., Teixeira, B.O., Pereira, G.A., 2019. GNSS/LiDAR-based navigation of an aerial robot in sparse forests. Sensors 19, 4061.

Corte, A.P.D., Souza, D.V., Rex, F.E., Sanquetta, C.R., Mohan, M., Silva, C.A., Zambrano, A.M.A., Prata, G., de Almeida, D.R.A., Trautenmüller, J.W., 2020. Forest inventory with high-density UAV-Lidar: Machine learning approaches for predicting individual tree attributes. Computers and Electronics in Agriculture 179, 105815.

Kelly, N., Di Tommaso, S., 2015. Mapping forests with Lidar provides flexible, accurate data with many uses. California Agriculture 69, 14-20.

Kukko, A., Kaijaluoto, R., Kaartinen, H., Lehtola, V.V., Jaakkola, A., Hyyppä, J., 2017. Graph SLAM correction for single scanner MLS forest data under boreal forest canopy. ISPRS journal of photogrammetry and remote sensing 132, 199-209.

Maitreya, A., Maitreya, A., Mankad, A., Modi, N., 2023. A review on carbon sequestration (non-destructive method) in urban ecosystem. International Association of Biologicals and Computational Digest 2, 245-252.

Novotny, J., Navratilova, B., Albert, J., Cienciala, E., Fajmon, L., Brovkina, O., 2021. Comparison of spruce and beech tree attributes from field data, airborne and terrestrial laser scanning using manual and automatic methods. Remote Sensing Applications: Society and Environment 23, 100574.

Otsu, N., 1979. A Threshold Selection Method from Gray-Level Histograms. IEEE Transactions on Systems, Man, and Cybernetics 9, 62-66.

Qian, C., Liu, H., Tang, J., Chen, Y., Kaartinen, H., Kukko, A., Zhu, L., Liang, X., Chen, L., Hyyppä, J., 2016. An integrated GNSS/INS/LiDAR-SLAM positioning method for highly accurate forest stem mapping. Remote Sensing 9, 3.

Ramezani, M., Khosoussi, K., Catt, G., Moghadam, P., Williams, J., Borges, P., Pauling, F., Kottege, N., 2022. Wildcat: Online continuous-time 3d lidar-inertial slam. arXiv preprint arXiv:2205.12595.

Safaie, A.H., Rastiveis, H., Shams, A., Sarasua, W.A., Li, J., 2021. Automated street tree inventory using mobile LiDAR point clouds based on Hough transform and active contours. ISPRS Journal of Photogrammetry and Remote Sensing 174, 19-34.

Shin, Y.-H., Shin, S.-Y., Rastiveis, H., Cheng, Y.-T., Zhou, T., Liu, J., Zhao, C., Varinlioğlu, G., Rauh, N.K., Matei, S.A., Habib, A., 2023. UAV-Based Remote Sensing for Detection and Visualization of Partially-Exposed Underground Structures in Complex Archaeological Sites. Remote Sensing 15, 1876.

Shu, D.Y., Deutz, S., Winter, B.A., Baumgärtner, N., Leenders, L., Bardow, A., 2023. The role of carbon capture and storage to achieve net-zero energy systems: Trade-offs between economics and the environment. Renewable and Sustainable Energy Reviews 178, 113246.

Su, Y., Guo, Q., Jin, S., Guan, H., Sun, X., Ma, Q., Hu, T., Wang, R., Li, Y., 2020. The development and evaluation of a backpack LiDAR system for accurate and efficient forest inventory. IEEE Geoscience and Remote Sensing Letters 18, 1660-1664.

Tang, J., Chen, Y., Kukko, A., Kaartinen, H., Jaakkola, A., Khoramshahi, E., Hakala, T., Hyyppä, J., Holopainen, M., Hyyppä, H., 2015. SLAM-aided stem mapping for forest inventory with small-footprint mobile LiDAR. Forests 6, 4588-4606.

Vinutha, H., Poornima, B., Sagar, B., 2018. Detection of outliers using interquartile range technique from intrusion dataset, Information and Decision Sciences: Proceedings of the 6th International Conference on FICTA. Springer, pp. 511-518.

Zhou, T., Ravi, R., Lin, Y.-C., Manish, R., Fei, S., Habib, A., 2023. In Situ Calibration and Trajectory Enhancement of UAV and Backpack LiDAR Systems for Fine-Resolution Forest Inventory. Remote Sensing 15(11), 2799.